Ain Shams Engineering Journal 11 (2020) 777–785

Contents lists available at ScienceDirect

Ain Shams Engineering Journal

journal homepage: www.sciencedirect.com

Engineering Physics and Mathematics

Biocompatible TiO_2-CeO_2 Nano-composite synthesis, characterization and analysis on electrochemical performance for uric acid determination

P. Parthasarathy *, S. Vivekanandan

School of Electrical Engineering, VIT University, Vellore, Tamilnadu, India

ARTICLE INFO

Article history:
Received 15 May 2019
Revised 22 October 2019
Accepted 15 November 2019
Available online 26 December 2019

Index terms:
Uric acid
Urease (Urs)
Glutamate dehydrogenase (GLDH)
Composite material
Electrochemical method

ABSTRACT

This study reports the development of a fast and facile route for the synthesis of novel TiO_2-CeO_2 nanocomposite film using sol-gel spin coating method with the mixture of commercial CeO_2, titanium-iso-propoxide (TTIP) and aqueous ammonia. Solutions of TTIP in ethanol were mixed with CeO_2 nanoparticles to form a mixed sol-gel. The sol containing TiO_2-CeO_2 was coated over the glass substrate and the resulting nanocomposite thin film were characterized in terms of phase and surface morphology by XRD, TEM, SEM and FT-IR. Conventional methods of the synthesis of CeO_2–TiO_2 nanocomposite require a long time, and TiO_2 is rarely found as a coated material. In contrast, the sol-gel spin coating method was able to synthesize CeO_2–TiO_2 sol within a very short time. The particle size of the TiO_2–CeO_2 nano-composite film was found to be 23 nm. The Uric acid biosensor was fabricated by immobilizing mixed enzyme [urease (Urs) and glutamate dehydrogenase (GLDH)] on this nano-composite film showed a response time of 10 s, sensitivity as 0.9016 μAcm^{-2} mM^{-1} and detection limit of 0.165 mM. The value of Michaelis–Menten constant (Km) estimated using Line weaver–Burke plot as 4.8 mM which indicates the high affinity of uricase towards its analyte (uric acid). The enhanced sensitivity and linear range of the nanobiocomposite film obtained by cyclic voltammetry measurements suggested that the mixed enzyme and TiO_2-CeO_2 composite material has novel characteristics for uric acid determination in the human blood for the application of arthritis diseases.

1. Introduction

The ongoing past has seen various examinations completed on advancement and enhancements for different highlights, for example, speed, selectivity and affectability, and decreased expense of electrochemical biosensors. Many metal oxide-based nano materials, for example, zinc oxide (ZnO), zirconium oxide (ZrO_2), tin oxide (SnO_2), titanium oxide (TiO_2), niobium oxide (Nb_2O_5) and cerium oxide (CeO_2) and so forth, have been utilized as immobilization frameworks for the improvement of biosensors [1]. Among those, nanostructured TiO_2 has gotten much consideration as an immobilization lattice for the structure of wanted biosensors on account of its one-dimensional nanostructure, electronic conductivity, and bigger explicit surface zone. It has been accounted for that the nearness of higher valence cationic (4 +) dopants upgrades the ionic conductivity of TiO_2 because of increment in the centralization of oxygen opening [2]. It was proposed that fractional introduction of TiO_2 nanoparticles may have an impact on ionic conductivity of this material close to the surface. These highlights are especially appealing as potential adsorbents for catalyst immobilization as encompassing temperature requires further improvement of new synergist materials with a high surface region and well-characterized responsive precious stone planes with predominant reactant movement [3].

Endeavors have as of late been made to tailor the catalytic properties of TiO_2 by the addition of CeO_2 to upgrade warm and electrical properties, and these novel materials have been misused for applications toward latent counter terminals and sensors. As of late, various sol-gel-determined oxide substrates were utilized for improving attributes of biosensors for recognition of different analytes. Different procedures, for example, radio frequency (RF) sputtering, electrochemical methods, and sol-gel methods, have been utilized for developing various composites. Among sol-gel

* Corresponding author.
E-mail address: arjunsarathii@gmail.com (P. Parthasarathy).
Peer review under responsibility of Ain Shams University.

Production and hosting by Elsevier

https://doi.org/10.1016/j.asej.2019.11.011

determined oxide substrates, TiO_2– CeO_2 films have obtained much consideration in biomedical applications because of different points of interest, for example, low temperature process capacity, extensive surface region, tunability, warm soundness, biocompatibility, and minimal effort [4–7]. Titanium oxide sol-gel films have been utilized to immobilize horseradish peroxidase (HRP) for application to H_2O_2 biosensor. What's more, sol-gel-inferred tin oxide/gelatin composite were utilized to examine direct electrochemistry and electro catalysis of horseradish peroxidase. Furthermore, this sol-gel-determined zirconia/Nafion composite has been utilized to manufacture glucose biosensor. Be that as it may, the above procedures need long response time. What's more, the immediate covering of TiO_2 on CeO_2 nanoparticles to nanocomposite has not been yet concentrated as far as we could possibly know. This is on the grounds that that arrangement of TiO_2-CeO_2 nanoparticles is troublesome utilizing the traditional techniques, and it is subsequently a test to locate a novel way to deal with [8].

Urea in blood or in urine is a significant analyte for the analysis of renal and liver maladies. The location of urea is performed every now and again in medicinal consideration. The ordinary dimension of urea in serum is in the range 2.5– 6.7 mM (15– 45 mg/dL) [9]. In patients experiencing renal malady, urea fixation in serum might be as high as 30– 80 mM requiring hemodialysis. An ongoing report from this research facility underpins the view that the electrochemical oxidation of uric corrosive at graphite and gold terminals continues by an underlying 2e- – 2H + response to give a diimine animal groups (Fig. 1). This diimine is truly precarious in fluid arrangement and is quickly hydrated to an imine-liquor in a first-request response [10]. The rate consistent and request for the last response were dictated by twofold potential advance chronoamperometric utilizing a profoundly cleaned wax-impregnated spectroscopic graphite anode. This anode was utilized to limit adsorption of the diimine which is especially serious at ordinary pyrolytic graphite cathodes. The rate consistent for hydration of the diimine to the imine-liquor at pH 8 was observed to be 32.5 s^{-1}. At lower and higher pH esteems this rate steady was in any event as huge as that saw at pH 8 [11,12]. The imine-liquor is additionally shaky yet it might be seen as an UV-engrossing middle of the road upon electrochemical oxidation of uric corrosive between pH 7–9 by methods for slight layer spectro electrochemical investigations.

A basic method of reasoning for our investigations of the electrochemical oxidation of naturally significant purine and different atoms is that such examinations can prompt data bearing on the response courses and systems of organic oxidation responses [13–17]. A basic schematic of electrochemical process over a graphite electrode is shown in the Fig. 1. In spite of the fact that there are still a few vulnerabilities with respect to the electrochemical oxidation of uric acid (e.g., the real structures of the diimine and imine-liquor intermediates) the essential response component is presently to a great extent comprehended. Likewise, an examination was started into the enzymatic oxidation of uric corrosive so as to create adequate information to look at the natural and electrochemical procedures. The organic oxidation of uric corrosive with different peroxidase proteins has likely been examined generally widely. Prior work has demonstrated that the items framed upon both electrochemical and enzymatic (peroxidase) oxidation of uric corrosive is the equivalent. In this way, at low pH the major electrochemical and enzymatic items are alloxan, urea and CO_2, while at middle of the road pH allantoin, urea and CO_2, are framed. The last laborers suggested that some obscure essential oxidation item is shaped which at that point experiences non-enzymatic, pH-subordinate decay to alloxan or allantoin.

Regularly, the task of uric corrosive biosensors depends either on the estimation of utilization of O_2 or generation of H_2O_2 in enzymatically catalyzed response. Uric corrosive biosensors of the last kind are winning because of their more straightforward development and shorter reaction time in contrast with the biosensors dependent on disintegrated oxygen tests. Since H_2O_2 is electro dynamic, these biosensors ordinarily utilize an amperometric transduction. Two issues are experienced being developed of amperometric uric corrosive biosensors dependent on electrochemical recognition of enzymatically created H_2O_2. The first is associated with the low explicit action of industrially accessible urate oxidase, which infrequently surpasses 20– 25 units for every mg and ordinarily is lower than 10 units for each mg, while the second is identified with the generally high ideal pH of urate oxidase, which lies close to the pH estimation of 9.0. Because of the low synergist movement of compound, the rate of H_2O_2 generation in enzymatically catalyzed response is low, bringing about the low current flag of the biosensor [18]. This puts the uncommon necessities on the H_2O_2 transducer utilized in the development of the biosensor. So as to acquire a low discovery limit and therefore, a wide unique scope of the biosensor, the transducer must display a high affectability and low commotion. The last can be accomplished if the biosensor is worked at gentle Cathodic possibilities (around 0.0 V versus Ag/AgCl), at which the foundation current is limited. In any case, because of the moderate energy of H_2O_2 decrease on the greater part of the usually utilized cathode materials, the considerable H_2O_2 decrease flows can be accomplished at these possibilities just on chemically adjusted terminals. As far as affectability and selectivity, a standout amongst the best inorganic impetuses for electrochemical decrease of H_2O_2 is Prussian blue (iron (III) hexacyanoferrate (II), KFe[Fe(CN)6]) [19–24].

The work reported here was undertaken to study the electrochemical behavior of uric acid in the presence of mixed enzymes such as urease and glutamate dehydrogenase. We have utilized sol-gel spin coating chemical process for thin film coating and cyclic voltammetry technique for electrochemical behavioral studies for the determination of uric acid in the presence of mixed enzyme in the catalytic reaction. Although many work relied on various types of polymers and other carbon based materials and less work in the metal oxide side, so in this work we synthesized a novel

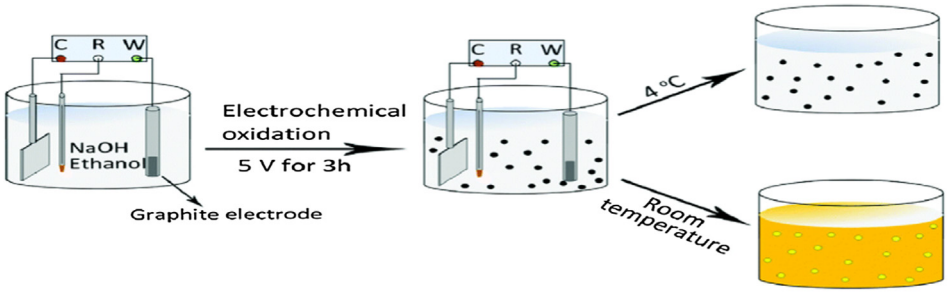

Fig. 1. Electrochemical reaction of uric acid at graphite electrodes [22].

metal oxide nanocomposite thin film for the detection of uric acid in the blood.

2. Experimental details

In the present work a novel Nanocomposite thin films exhibiting good electron transfer property has been developed by Sol-Gel spin coating technique for the detection of uric acid. Mixed enzyme is successfully immobilized on the surface of TiO_2-CeO_2 thin film matrix by physical adsorption process and enhanced bio-sensing response characteristics of the prepared bio-electrode for uric acid have been achieved.

2.1. Materials

TTIP, (99.0%), aqueous ammonium NH_4OH (28–30%), $Ce(NO_3)_3$·$6H_2O$ (CAS number 10294–41-4), Urease (Urs), glutamate dehydrogenase (GLDH), nicotinamide adenine dinucleotide (NADH) a-keto glutarate (a-KG), ethanol, HNO3 and other solvents, and reagents were procured from purchased from Sigma Aldrich and Merck India Ltd., Mumbai, India. Indium tin oxide (ITO)-coated glass substrates were used here. All other chemicals were of reagent grade and were used without further purification. Milli-Q water was used in all the preparations.

2.2. Synthesis of mixed metal oxide nano-particles

The mixed metal oxide nanoparticles were synthesized using a sol-gel method and the flow chart for the synthesis was depicts below (Fig. 2).

Briefly, TTIP and ethanol were added together with few drops of H_2O and it is mixed in a beaker under magnetic stirring to obtain a homogeneous precursor solution as TiO_2 sol. Then obtained TiO_2 sol is mixed with mixture solution of cerium nitrate and ethanol as a precursor to get the CeO_2 sol. The total solution is continuously stirred under room temperature continuously for 2 h. Here acetic acid is added in few drops and it acts as a catalyst and it is left stirring for 1 h at room temperature. Subsequently, the solution containing TiO_2- CeO_2 was left for aging overnight to obtain the mixed sol-gel metal oxide nanocomposite. The formation of nanocomposite and its chemical reaction is shown in the below Fig. 3.

2.3. Sol-gel derived tio2-ceo2 films preparation

Mixed TiO_2–CeO_2 sol-gel was deposited on pre cleaned ITO-coated glass substrates by using the spin-coating technique with a rotating speed of 300 rpm. These films were preheated at 200 °C for about 5 min in air for oxide formation. The grown TiO_2–CeO_2 thin films were found to be amorphous which becomes a nano-crystalline after a post deposition annealing treatment at 300 °C for 1 h in atmospheric air. The annealed thin films were found to be smooth, transparent and strongly adherent to the substrate.

2.4. Electrode modification and immobilization of urease

Ten microliters (μL) of 1:1 M mixture of urease and GLDH (1.0 mg/mL, in PB, 50 mM and pH 7.0) was immobilized onto a TiO_2–CeO_2 nanocomposite film by the Physisorption method. The biochemical reaction using the mixed enzyme system is shown below. The general schematic of enzyme immobilized over the electrode surface is shown below (Fig. 4).

$$Urease \rightarrow 2NH_4^+ + HCO_3^- \quad (1)$$

$$2NH_4^+ + \alpha - Ketoglutamate + NADH \rightarrow GLDH2 - Glutamate + NADH^+ \quad (2)$$

$$NADH \rightarrow NAD^+ + 2e^- \quad (3)$$

The enzyme solution was poured onto TiO_2–CeO_2 films and kept for approximately 4 h in a humid chamber at room temperature for uricase binding. The bio electrode (Urs-GLDH/TiO_2–CeO_2/ ITO) was washed thoroughly with phosphate buffer solution to remove any unbound enzyme and was stored at room temperature when not in use. The prepared bio electrode (Urs-GLDH/TiO_2–CeO_2/ ITO) was allowed to dry overnight under desiccated conditions and then washed with phosphate buffer saline (PBS, 50 mM, pH 7.0, 0.9% NaCl) to remove any unabsorbed enzymes (Urs-GLDH) and stored in a desiccator at 25 when not in use. To obtain a uniformly distributed OH group on thin film surface, the films were immersed in a solution of H_2O_2/NH_4OH/ H_2O (1:1:5, v/v) for 30 min at 80 for hydrolysis, after which they were rinsed thoroughly with de-ionized water and dried.

2.5. Sensing principle

Uricase catalyzes the in vivo oxidation of uric acid ($C_5H_4N_4O_3$) in the presence of oxygen to produce allantoin ($C_4H_6N_4O_3$) and CO_2 as oxidation products of uric acid and hydrogen peroxide as a reduction product of O_2. The below Fig. 5 demonstrated the basic schematic of uricase catalytic reaction and its chemical reaction is as follows:

$$UricAcid(C_5H_4N_4O_3) + H_2O + O_2 \rightarrow Allantoin(C_4H_6N_4O_3) + CO_2 + H_2O_2 \quad (4)$$

$$H_2O_2 \rightarrow O_2 + 2H^+ + 2e^- \quad (5)$$

The enzymatic electrochemical biosensor relies on shuttling of these electrons, generated in the biochemical reaction shown above, from the redox center of the enzyme to the electrode via Nanocomposite thin film matrix. Enzymes, because of their insulated-shell redox centers, are unable to show direct electrochemistry. The presence of a redox species (mediator $[Fe(CN)_6]^{3-/4-}$), in the system, provides the path for electron transfer from the redox centers of the enzyme to the electrode using good electron communication property of the prepared TiO_2-CeO_2 thin film matrix, which results in increase in peak oxidation and reduction currents. The current further increases linearly with the increase in the concentration of analyte (uric acid) in the solution.

3. Result and discussion

Phase identification of the fabricated sol-gel-derived TiO_2–CeO_2 Nano-composite film was accomplished by X-ray Difractometer using Cu Ka radiation. These sol-gel-derived TiO_2–CeO_2/ITO and Urs-GLDH/TiO_2–CeO_2/ITO bio electrodes were further characterized by Fourier transform infrared (FTIR) spectrophotometer in the spectral range 400–4000 cm^{-1}. Atomic force microscopy (AFM), SEM and TEM was used to examine the surface roughness and surface morphology of TiO_2–CeO_2 nanocomposite films. Electrochemical data was obtained on an Auto lab Potentiostat/Galvanostat using a three-electrode cell containing Ag/AgCl as reference electrode, platinum (Pt) wire as auxiliary electrode, and Urs-GLDH/TiO_2–CeO_2/ITO bio electrodes as a working electrode.

3.1. XRD Analysis

Fig. 6 shows the results of the x-ray diffraction (XRD) studies in intensity range 20–70° of the TiO_2–CeO_2 film deposited on ITO

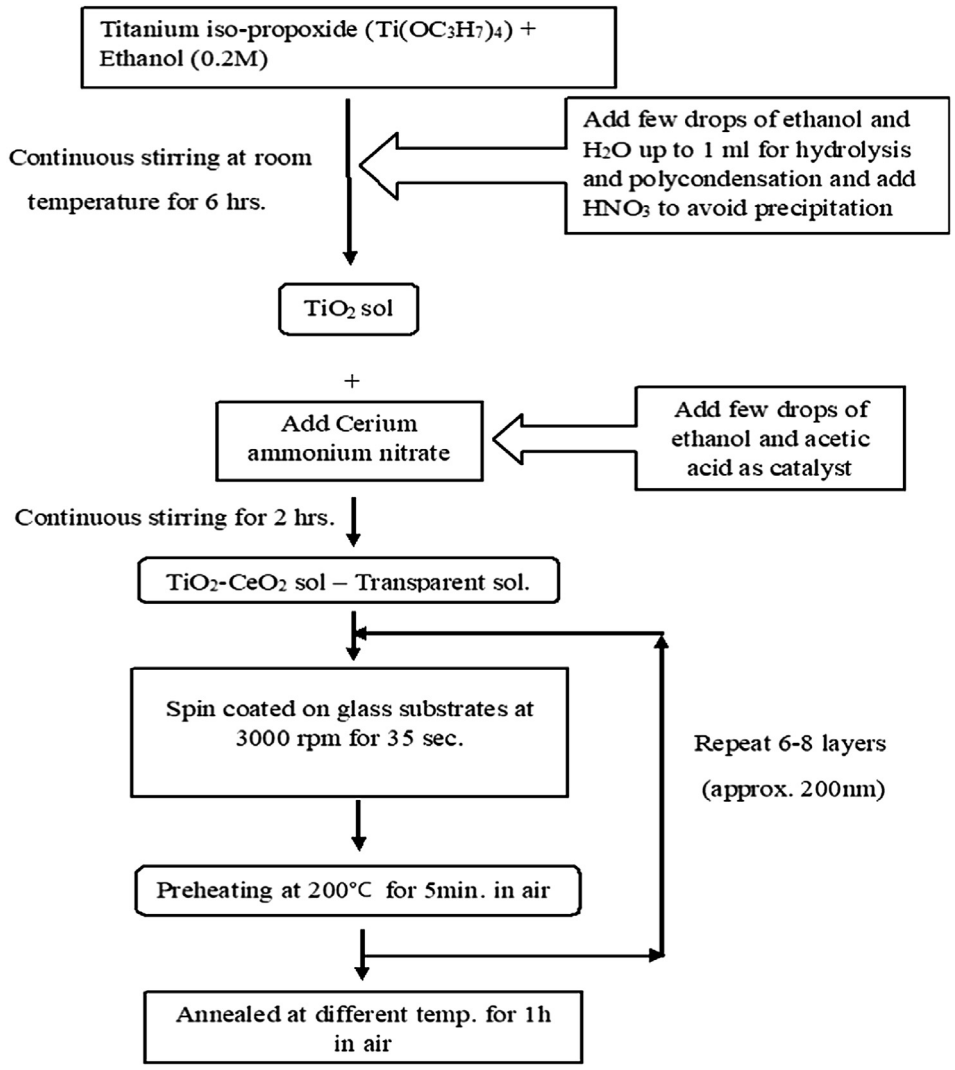

Fig. 2. TiO_2–CeO_2 thin film formation flow chart.

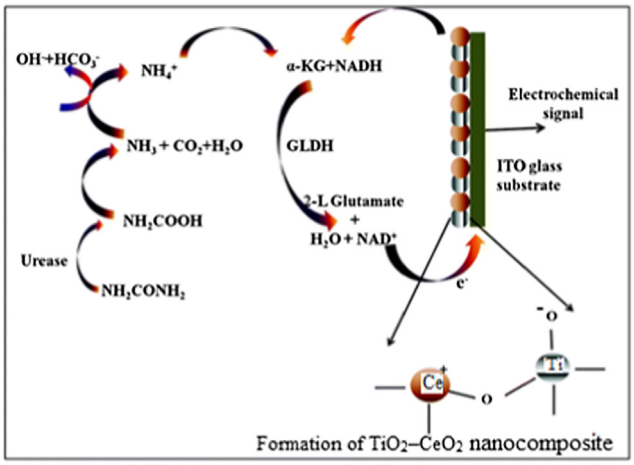

Fig. 3. TiO2–CeO2 nanocomposite formation reaction.

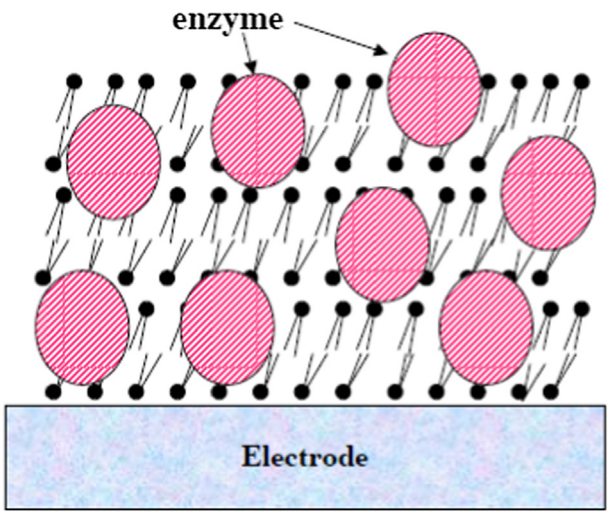

Fig. 4. General schematic of enzyme immobilized over the electrode surface.

glass substrate through the sol-gel chemical process calcinated at 200 . The XRD pattern of CeO_2-TiO_2 metal oxide nano-composite is shown below with the peaks appeared at 28.57°, 33.14°, 47.52°, 56.46° and 59.20°. It is shows that the mentioned peaks are mixed phase of three different phase of TiO_2 and the average crystallite size was estimated by the analysis of the broadening of (1 1 1) and (2 0 0) reflections and was found to be 23 nm. The

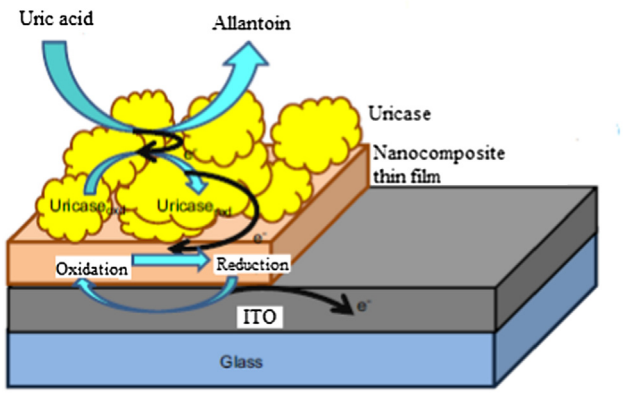

Fig. 5. Basic schematic of Uricase catalytic reaction.

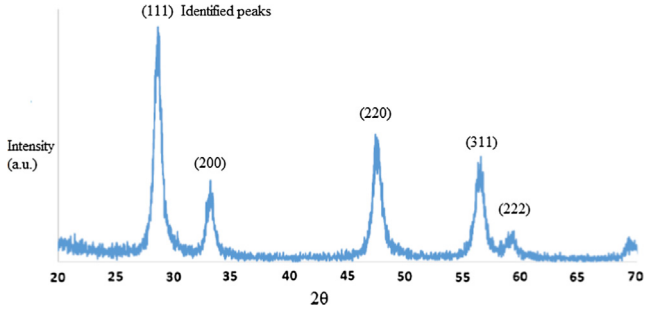

Fig. 6. X-ray diffraction (XRD) of TiO2–CeO2 nanocomposite.

lattice constant (a) of the TiO_2 film calculated from the peak position (1 1 1) found to be (a) = 0.460 A°, is slightly higher than that of bulk TiO2 (0.455 A °) and is assigned to the distortion in the unit cell along the growth direction. In addition, an increase in the lattice constant reveals the lattice expansion effect resulting from the substitution of Ce4 + ions with decreasing particle size. The results imply that Ti atoms substitute Ce4 + ion in the TiO_2 lattice.

3.2. Sem analysis

The SEM micrograph (Fig. 7a and b) implies that the synthesized TiO_2 and TiO_2–CeO_2 nanocomposite thin films grown on ITO glass substrate have uniform morphologies and high aspect ratios with an average diameter of 600 nm and a length of 60–90 μm with uniform distribution of nanostructured grains. The grain size of the TiO_2 and TiO_2–CeO_2 is found as around 13 nm and 34 nm respectively. As the average crystallite size calculated from the XRD is in the same range, we are getting exact information on about the surface morphology of the sample from SEM micrograph.

3.3. TEM Analysis

The corresponding TEM images are shown in the below Fig. 8. The average crystallite size calculated from TEM images was found to be 10.2 ± 2.2 nm, which is in good agreement with the XRD result. In accordance with the small crystalline size, a large BET surface area of 78.6 $m^2\ g^{-1}$ was obtained. If these results are compared with those obtained from pristine CeO2 (55.7 $m^2\ g^{-1}$), which was reported in some studies, it was seen that the modification of CeO2 lattice with Ti^{4+} ions yielded a larger surface area.Fig. 9.

3.4. FTIR analysis

The TiO_2–CeO_2/ITO and Urs-GLDH/ TiO_2–CeO_2/ITO bio-electrodes characterized by FTIR spectroscopy are shown in the below figure. The bending and stretching vibrations of the hydroxyl (O–H) group corresponds to the bands formed at 1414 and 1530 cm^{-1} (weak band) and 3352 cm^{-1} (diffuse band). The appearance of these bands suggests the adsorption of moisture on the surface of nanostructured films. The deposition of TiO_2–CeO_2 film on the ITO surface confirms by having the intense and sharp band at around 448 cm^{-1}. Also the bands formed at 1928, 1616, 1525, and 1019 cm^{-1} corresponding to the stretching and bending vibrations indicating mixed enzyme immobilization on the nanocomposite thin film matrix. FTIR results indicate Urs-GLDH binding with the nanocomposite via electrostatic interaction and hydrogen bond formation. The shift of the Ti–O–Ce stretching band toward a higher wave number (456 cm^{-1}) may be attributed to the electrostatic interaction and hydrogen bonding of the ceramic nanocomposite with the enzymes (Urs-GLDH).

3.5. AFM Analysis

The AFM micrographs (Fig. 10a and 10b) show surface topography of the prepared TiO_2–CeO_2 film revealing formation of the uniformly distributed spherical nanostructured thin film. The surface roughness of the TiO_2–CeO_2/ITO film determined as root mean square (RMS) = 52 nm indicates high porosity and it increases to 5 nm after enzyme (Urs-GLDH) immobilization. Globular structure is due to the presence of Urs-GLDH on the bio-electrode surface.

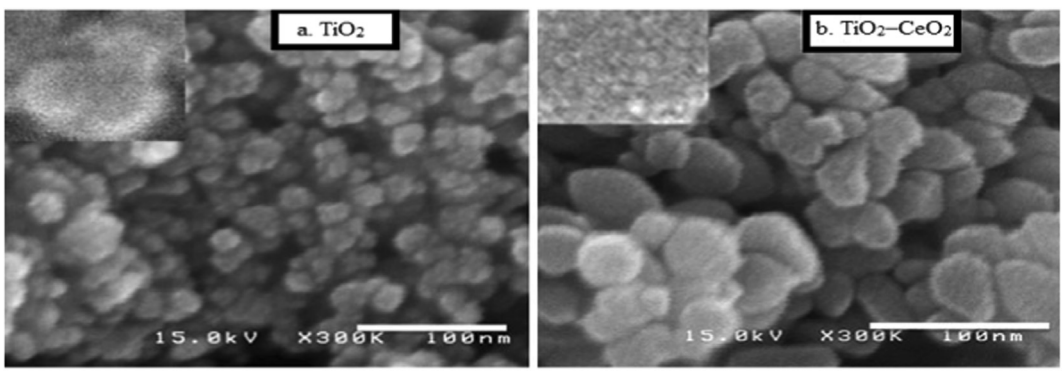

Fig. 7. SEM images of (a) TiO2 thin film and (b) TiO2–CeO2 nanocomposite thin film.

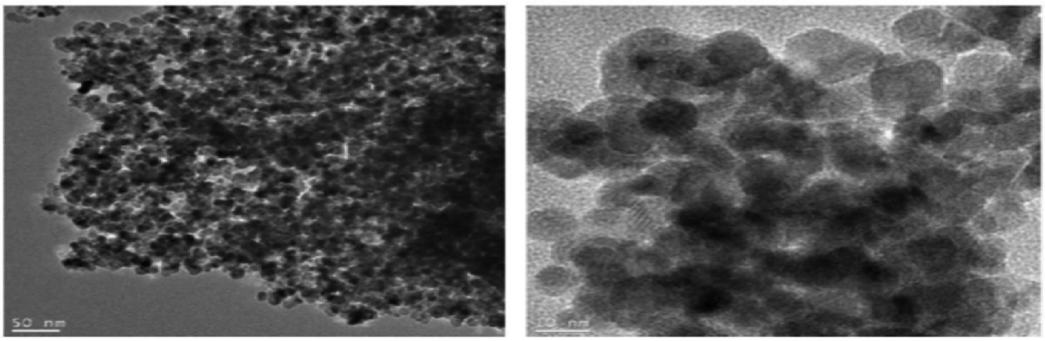

Fig. 8. TEM images of TiO2 and TiO2–CeO2 at different magnification.

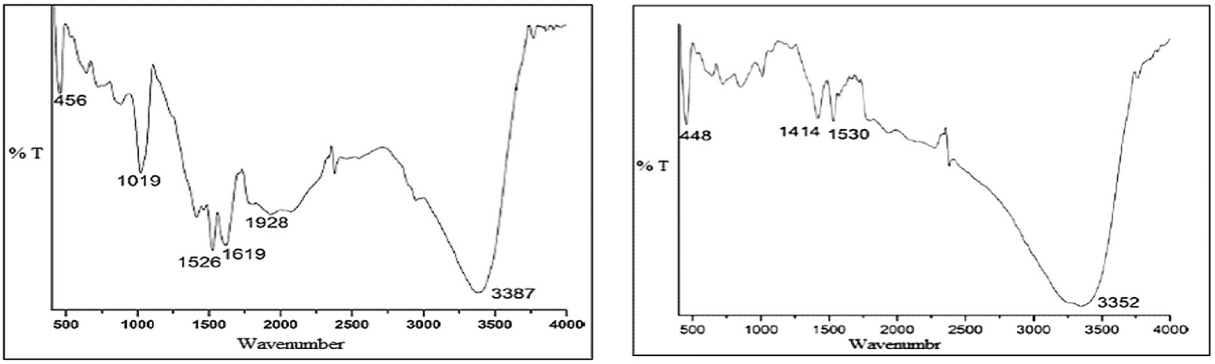

A. FTIR Spectra of Sol-gel derived TiO_2–CeO_2/ITO nanocomposite film

B. FTIR Spectra of Urs-GLDH/TiO_2–CeO_2/ITO bioelectrode film

Fig. 9. A. FTIR Spectra of TiO2–CeO2/ITO nanocomposite film and 8. B. FTIR Spectra of Urs-GLDH/ TiO2–CeO2/ITO bio-electrodes.

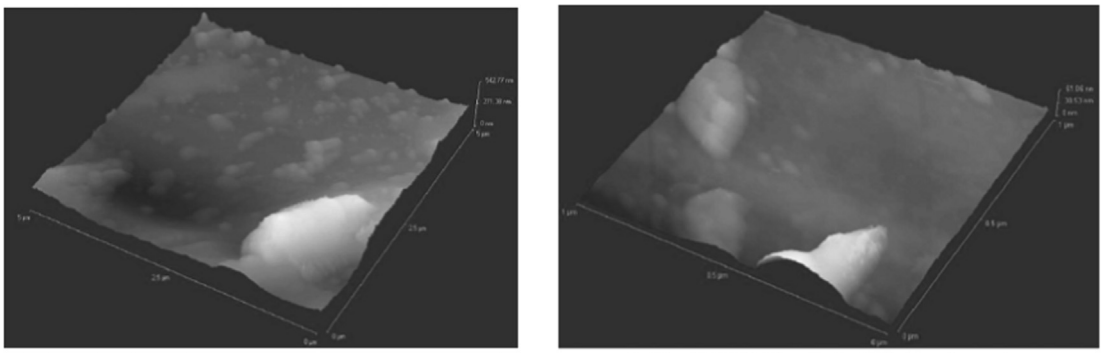

A. Sol-gel derived TiO_2–CeO_2/ITO nanocomposite electrode

B. Urs-GLDH TiO_2–CeO_2/ITO bio-electrode

Fig. 10. A. AFM image of TiO2–CeO2/ITO nanocomposite film and 10. B. AFM Image of Urs-GLDH/ TiO2–CeO2/ITO bio-electrodes.

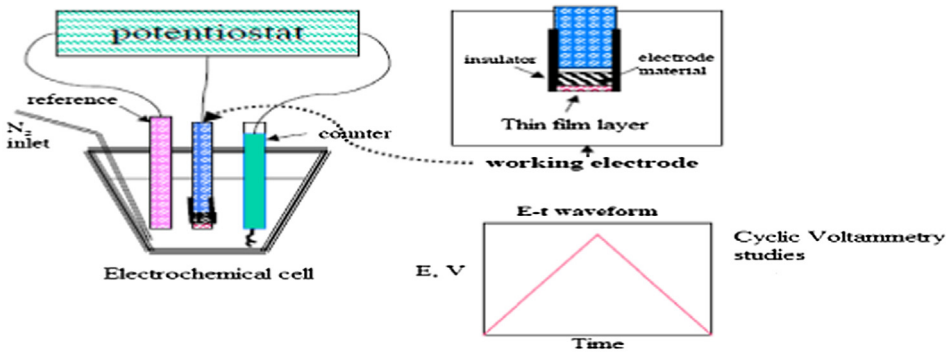

Fig. 11. Graphical measurement setup for Cyclic Voltammetry studies [19].

3.6. Electrochemical study

The electrochemical performance of the sensors was evaluated using a 3-electrode electrochemical cell. 0.01 M PBS solution with the pH of 7.4 was used as the electrolyte

(Graphical setup Fig. 11). The experiments were carried out using a Biologic SP-150 Potentiostat. Pt wire and Ag/AgCl electrodes were used as counter and reference electrodes, respectively. The laboratory setup is shown in below Fig. 12. The term of sensitivity employed in the manuscript defines the surface area-normalized sensitivity values. The constructed sensor was named as the Urs-GLDH/ TiO_2–CeO_2/ITO bio-electrode.

(1) Electrochemical performance analysis

The electrochemical property of Urs-GLDH/TiO_2– CeO_2/ITO biosensors was assessed utilizing cyclic voltammetry (CV) directed in 0.01 M PBS. The CV bends of uncovered Pt and Urs-GLDH/TiO_2–CeO_2/ITO electrodes recorded in the range of 5 mM uric acid are appeared in Fig. 13. It was seen that exposed Pt terminal did not show any adjustment in the CV bend after the expansion of 5 mM uric acid into the electrolyte, demonstrating that Pt surface did not have any electrochemical action towards uric acid. Then again, when the outside of the electrode was changed with nanocomposites and the catalyst layer, the terminal showed a noteworthy increment in the oxidation current within the sight of 5 mM uric acid. The oxidation began at around 0.3 V was because of the oxidation of H_2O_2 on the outside of the cathode·H_2O_2 oxidized on the terminal surface was delivered from the enzymatic response (Eq. (1)). Moreover, the oxidation response of H_2O_2 on the terminal surface is appeared in Eq. (2). Accordingly, the CV bends affirmed that the developed sensors demonstrated a huge reaction to the expansion of uric corrosive into the PBS arrangement (Eq. (2)).

An electrochemical response examination of Urs-GLDH/TiO2–CeO2/ITO bio-cathode has been driven as a part of urea in closeness of NADH just as α-KG in PBS using CV. The measure of response peak current augmentations as urea center additions. In proposed biochemical reaction urease enlivens urea hydrolysis to carbamine destructive which gets hydrolyzed to smelling salts (NH_3) and carbon dioxide (CO_2). GLDH catalyzes the revocable reaction between α-KG and NH3 to NAD + and associated oxidative deamination of L-glutamate in two phases. The underlying advance incorporates a Schiff base widely appealing molded among NH3 and α-KG (Step A). By then Schiff base center protonated in light of trade of the hydride particles from NADH realizing advancement of L-glutamate (Step B). NAD + is utilized in the forward reaction of α-KG and free NH_3 that is changed over to L-glutamate by methods for hydride trade from NADH to glutamate. NAD + is utilized in the turnaround reaction, including L-glutamate being changed over to α-KG and free (NH3) by methods for oxidative reaction. The made electrons in the midst of the above reactions are traded to TiO_2–CeO_2/ITO anode.

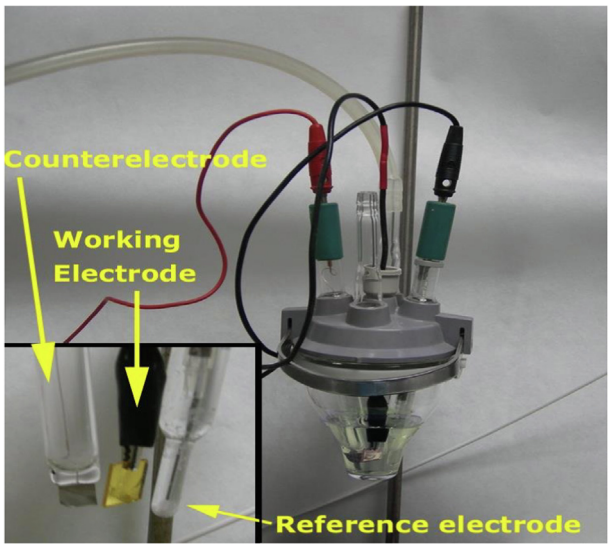

Fig. 12. Laboratory measurement setup for Cyclic Voltammetry studies.

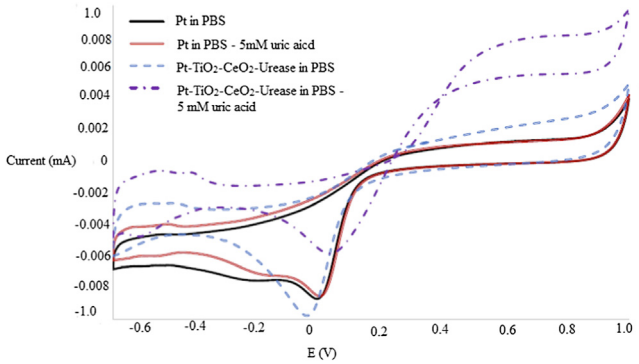

Fig. 13. The CV curves of bare Pt and Pt/CeO2-TiO2/Urs/GLDH in the absence and presence of 5 mM uric acid (10 mV s-1, 0.01 M PBS, pH: 7.4).

$$(NH_2)_2CO + 3H_2O \overset{urease}{\rightarrow} 2NH_4^+ + OH^- + HCO_3^- StepA \quad (6)$$

$$NH_4^+ + \alpha - ketoglutarate + NADH \overset{GLDH}{\rightarrow} L - glutamate + NAD^+ + 2e\ \ stepB \quad (7)$$

(2) Effect of scan rate

The effect of the scan rate on the electrochemical performance of the sensors was evaluated by conducting the CV experiments at various scan rates between 10 and 300 mV s-1. The scan rate vs. oxidation current graph is shown in Fig. 14. It was found that the oxidation current of Urs-GLDH/ TiO_2–CeO_2/ITO sensors measured at 0.8 V increased linearly with the increasing scan rate as shown in Fig. 15, demonstrating that the oxidation of H_2O_2 on the surface of the sensor is a surface controlled electrochemical reaction.

The presentation of the constructed biosensors was assessed utilizing chronoamperometric technique directed in 0.01 M PBS at the pH of 7.4. The CV aftereffects of the sensors were considered so as to decide the ideal working potential. As appeared in Fig. 14, the oxidation of H_2O_2 began at the capability of 0.3 V, and a further

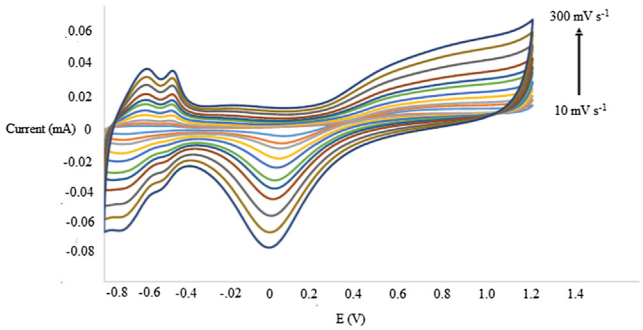

Fig. 14. Effect of scan rate on the electrochemical performance of Urs-GLDH/ TiO2–CeO2/ITO sensors biosensors.

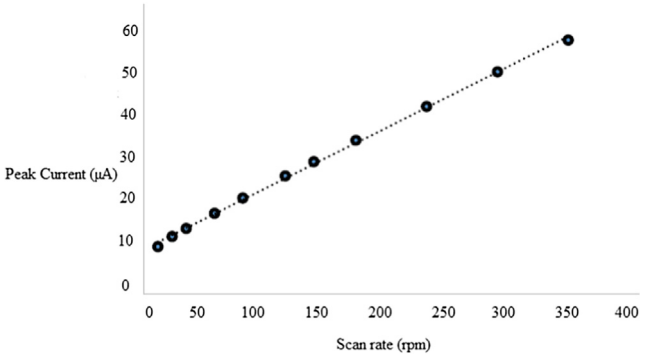

Fig. 15. Peak current vs. scan rate.

increment in the connected voltage yielded higher oxidation current. In spite of the fact that the expansion in the connected voltage brought about a noteworthy increment in the reaction current up to 0.6 V, further increment in the voltage did not influence the pinnacle current to a similar degree because of achieving a level at around 0.8 V. Consequently, the ideal working potential for the chronoamperometric tests was picked as 0.6 V.

The chronoamperometric consequences of Urs-GLDH/TiO_2–CeO_2/ITO based biosensors are appeared in Fig. 16. As observed from Fig. 16, when 20 μM of uric corrosive was infused into the electrolyte, a quick increment in the current was watched, demonstrating the location of uric corrosive brought into the PBS arrangement. The reaction current achieved a steady an incentive in a short measure of time (<5s), which affirmed the short reaction time of the built sensors. The current-focus diagram acquired from progressive expansion of 20 μM of uric corrosive is appeared underneath figure. The affectability of the biosensors was observed to be 0.085 ± 0.008 μA μM-1 cm-2 (n = 5). So as to show the reproducibility of the biosensor creation process, the RSD % esteem was determined utilizing various biosensors (n = 3). The outcomes demonstrated a RSD % of 1.3 appearing brilliant reproducibility of the manufacture procedure.

The linear range of the biosensors was dictated by the progressive expansion of 50 μM uric corrosive into the PBS arrangement, and the acquired I-t curve is appeared in Fig. 17. It was seen that the progressive expansion of 50 μM uric corrosive delivered a direct increment in the reaction current up to 0.6 mM. The further increment in the focus, be that as it may, brought about a deviation from linearity of sensor reaction. At the point when the current-fixation charts appeared in Figs. 15 and 16 are considered, it was reasoned that the built biosensors demonstrated a straight range between 20 μM and 600 μM towards the recognition of uric acid.

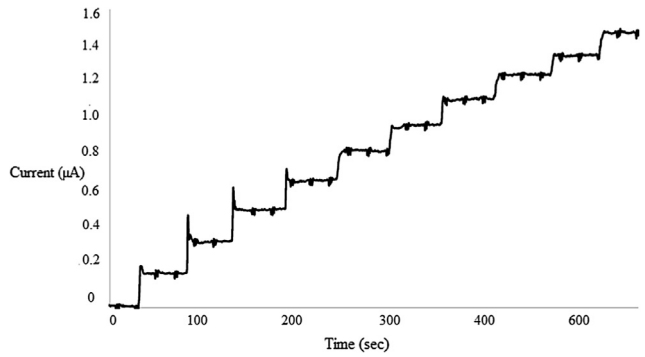

Fig. 16. Amperometric response of Urs-GLDH/ TiO_2–CeO_2/ITO biosensor to the successive addition of 20 μM uric acid into the PBS solution at the working potential of 0.6 V.

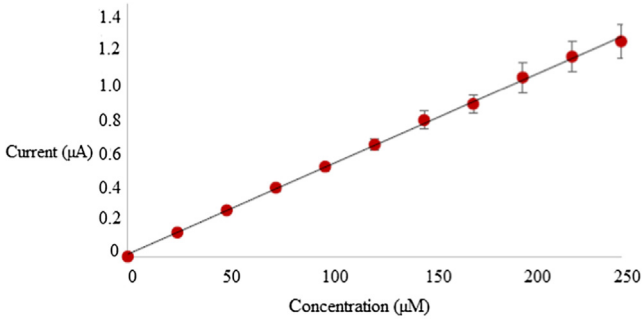

Fig. 17. Current vs. concentration graph.

(3) Response characteristics of biosensor

Fig. 13 shows the reaction of the Urs-GLDH/TiO_2-CeO_2/ITO biocathode in PBS arrangement within the sight of NADH and a-KG and a progressive expansion of urea at a connected 50 mV/s examine rate. The pinnacle current ascents forcefully with expanded centralization of urea, with the greatest reaction approach at the convergence of 700 mg/dL after which it diminishes. The sensor accomplishes 95% of the unfaltering state current in under 5 s demonstrating quick electron trade between the Urs-GLDH and TiO_2– CeO_2/ITO cathode. From the plot, two direct ranges are gotten for recognition of urea (Fig. 17). The anode is observed to be direct in the range 10– 100 mg/dL and 100– 700 mg/dL (Fig. 18) with affectability of 0.078 mAcm-2 mM-1 and 0.901 mA cm^{-2} mM^{-1} and relationship coefficients R = 0.999 and 0.994, individually, and the location furthest reaches of 0.166 mM with a relative standard deviation of 0.0022% utilizing the Lineweaver– Burke Equation underneath

$$\frac{I}{I_{ss}} = \frac{1}{I_{maxx}} + \frac{K_m^{qpp}}{I_{maxx}^{c}} \tag{8}$$

where I_{ss} is the steady-state current after the addition of substrate

C is the bulk concentration of the substrate

I_{maxx} is the maximum current measured under saturated substrate condition

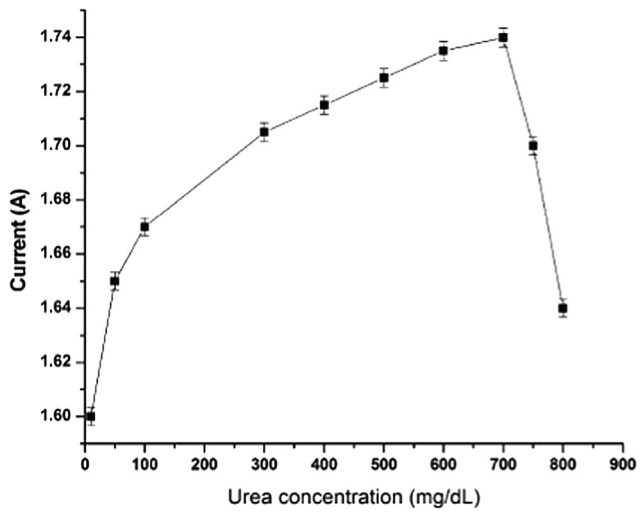

Fig. 18. Response characteristics curve of bio-sensor.

4. Conclusion

In this work, we structured novel electrochemical biosensors for the recognition of uric acid by immobilizing a mixed enzyme Urease and GLDH blended catalyst onto the TiO_2– CeO_2 nanocomposite film by exploiting the extensive surface region and high synergist action of CeO_2-TiO_2 blended metal oxide nano-composites. In the initial segment of the examination, CeO_2-TiO_2 nanocomposites was synthesized effectively. The normal molecule size of the nano-composite was observed to be 23 nm, additionally affirmed by SEM and AFM pictures and the electrochemical presentation of these sensors was examined utilizing Cyclic Voltammetry strategy. This biosensor displays brilliant performances, for example, sensitivity (0.9016 $mAcm\text{-}^{2}mM^{-1}$) and reproducibility, wide linear range (10– 700 mg/dL), low identification limit (0.165 mM). At the point when the exhibition of the built sensors was contrasted and the writing, it was seen that one of the most astounding sensitivity esteems was acquired from our novel sensor. The outcomes recommended that CeO_2-TiO_2 blended metal oxide nano-composites are promising materials which can be effectively used to create enzymatic electrochemical sensors with upgraded execution.

References

[1] Wang J. Electrochemical glucose biosensors. Chem. Rev. 2007;108:814.
[2] Lee H, Yoon SW, Kim EJ, Park J. In-situ growth of copper sulfide nanocrystals on multiwalled carbon nanotubes and their application as novel solar cell and amperometric glucose sensor materials. Nano Lett. 2007;7:778.
[3] Singh SP, Arya SK, Pandey P, Malhotra BD, Saha S, Sreenivas K, et al. Cholesterol biosensor based on rf sputtered zinc oxide nanoporous thin film. Appl. Phys. Lett. 2007;91:063901.
[4] Parthasarathy P, Vivekanandan S. A comprehensive review on thin film-based nano-biosensor for uric acid determination: arthritis diagnosis. World Rev Sci Technol Sust Develop 2018;14(1):52–71.
[5] Khan R, Kaushik A, Solanki PR, Ansari AA, Pandey MK, Malhotra BD. Zinc oxide nanoparticles-chitosan composite film for cholesterol biosensor. Anal. Chim. Acta 2008;616:207.
[6] Parthasarathy P, Vivekanandan S. Urate crystal deposition, prevention and various diagnosis techniques of GOUT arthritis disease: a comprehensive review. Health Inform Sci Syst 2018;6(1):19.
[7] Ghodsi FE, Tepehan FZ, Tepehan GG. Influence of pH on the optical and structural properties of spin coated CeO2–TiO2 thin films prepared by sol-gel process. Surf. Sci. 2007;601:4497.
[8] Gambhir M, Gerard AK Mulchandani, Malhotra BD. Co-immobilization and characterization of urease and glutamate dehydrogenase in electro-chemically prepared polypyrrole-polyvinylsulphonate films. Appl. Biochem. Biotechnol. 2001;96:249.
[9] Zhang Y, He P, Hu N. Horseradish peroxidase immobilized in TiO2 nanoparticle films on pyrolytic graphite electrodes: Direct electrochemistry and bioelectrocatalysis. Electrochim. Acta 2004;49:1981.
[10] Kim HJ, Yoon SH, Choi HN, Lyu YK, Lee WY. Amperomatric glucose biosensor based on sol-gel derived zirconia/ nafion composite film as encapsulation matrix. Bull. Korean Chem. Soc. 2006;27:65.
[11] Wang JX, Sun XW, Wei A, Lei Y, Cai XP, Li CM, et al. Zinc oxide nanocomb biosensor for glucose detection. Appl. Phys. Lett. 2006;88:233106.
[12] Yang Y, Yang H, Yang M, Liu Y, Shen G, Yu R. Amperometric glucose biosensor based on a surface treated nanoporous ZrO2/Chitosan composite film as immobilization matrix. Anal. Chim. Acta 2004;525:213.
[13] Parthasarathy P, Vivekanandan S. A numerical modelling of an amperometric-enzymatic based uric acid biosensor for GOUT arthritis diseases. Inf Med Unlocked 2018;12:143–7.
[14] Zong S, Cao Y, Zhou Y, Ju H. Zirconia nanoparticles enhanced grafted collagen tri-helix scaffold for unmediated biosensing of hydrogen peroxide. Langmuir 2006;22:8915.
[15] Parthasarathy P, Vivekanandan S. Investigation on uric acid biosensor model for enzyme layer thickness for the application of arthritis disease diagnosis. Health Inform Sci Syst 2018;6:1–6.
[16] Shi YT, Yuan R, Chai YQ, He XL. Development of an amperometric immunosensor based on TiO2 nanoparticles and gold nanoparticles. Electrochim. Acta 2007;52:3518.
[17] Parthasarathy P, Vivekanandan S. A typical IoT architecture-based regular monitoring of arthritis disease using time wrapping algorithm. Int J Comput Appl 2018:1–11.
[18] Xu X, Tian B, Zhang S, Kong J, Zhao D, Liu B. Electrochemistry and biosensing reactivity of heme proteins adsorbed on the structure-tailored mesoporous Nb2O5 matrix. Anal. Chim. Acta 2004;519:31.
[19] Parthasarathy P. Synthesis and UV detection characteristics of TiO2 thin film prepared through sol gel route. In: IOP conference series: materials science and engineering. (Vol. 360, No. 1). IOP Publishing; 2018, p. 012056.
[20] Feng KJ, Yang YH, Wang ZJ, Jiang JH, Shen GL, Yu RQ. A nano-porous CeO2/Chitosan composite film as the immobilization matrix for colorectal cancer DNA sequenceselective electrochemical biosensor. Talanta 2006;70:561.
[21] Yu J, Ju H. Preparation of porous titania sol-gel matrix for immobilization of horseradish peroxidase by a vapor deposition method. Anal. Chem. 2002;74:3579.
[22] Suzuki T, Kosacki I, Anderson HU. Defect and mixed conductivity in nanocrystalline doped cerium oxide. J. Am. Ceram. Soc. 2002;85:1492.
[23] Kosacki I, Suzuki T, Petrovsky V, Anderson HU. Electrical conductivity of nanocrystalline ceria and zirconia thin films. Solid State Ionics 2000;136–137:1225.
[24] Nakagawa K, Murata Y, Kishida M, Adachi M, Hiro M, Susa K. Formation and reaction activity of CeO2 nanoparticles of cubic structure and various shaped CeO2–TiO2 composite nanostructures. Mater. Chem. Phys. 2007;104:30.

Parthasarathy Panchatcharam. Parthasarathy is a Research Associate currently pursuing PhD in VIT University where his research interest mainly focused on sensor development for some real time applications in environmental and medical fields. He received his Master's in Sensor System Technology at VIT University, India in 2016 and Bachelors in Electronics and Instrumentation Engineering in Anna University, Chennai in 2013. His area of interest and research lies in nano materials for the development of sensors for medical application, industries and environmental applications, internet of things, IoMT, Machine learning, Big data and Health data analytics. He has published various research papers in the reputed international journals and conferences. He is a life time member in the professional societies like ISA, IETE, etc. He currently working in the field of biosensors and IoT based healthcare devices and had a passion for interdisciplinary approaches to solve the technical and analytical challenges.

S Vivekanandan. He is currently working as an Associate professor in the school of Electrical Engineering, VIT University, Vellore. He received his Ph.D. in 2014 from VIT University. He is an author and co-author of many research and review article in various international journal. He is Faculty coordinator for ISA Student section-District 14 and also received best mentor award in the year 2017.